

The solar bolometric imager

P.N. Bernasconi ^{a,*}, H.A.C. Eaton ^a, P. Foukal ^b, D.M. Rust ^a

^a *JHU Applied Physics Laboratory, 11100 Johns Hopkins Road, Laurel, MD 20723-6099, USA*

^b *192 Willow Road, Nahant, MA 01908, USA*

Received 19 October 2002; received in revised form 28 August 2003; accepted 29 August 2003

Abstract

The balloon-borne Solar Bolometric Imager (SBI) will provide the first bolometric (integrated light) maps of the solar photosphere. It will evaluate the photometric contribution of magnetic structures more accurately than has been possible with spectrally selective imaging over restricted wavebands. More accurate removal of the magnetic feature contribution will enable us to determine if solar irradiance variation mechanisms exist other than the effects of photospheric magnetism. The SBI detector is an array of 320×240 ferro-electric thermal IR elements whose spectral absorptance has been extended and flattened by a deposited layer of gold-black. The telescope itself is a 30-cm Dall–Kirkham design with uncoated primary and secondary pyrex mirrors. The combination of telescope and bolometric array provides an image of the Sun with a flat spectral response between 0.28 and $2.6 \mu\text{m}$, over a field of view of 917×687 arcsec, and a pixel size of 2.8 arcsec. After a successful set of ground-based tests, the instrument is being readied for a one-day stratospheric balloon flight that will take place in September 2003. The observing platform will be the gondola previously used for the Flare Genesis Experiment (FGE), retrofitted to house and control the SBI telescope and detector. The balloon flight will enable SBI to image over essentially the full spectral range accepted by non-imaging space-borne radiometers such as ACRIM, making the data sets complementary. The SBI flight will also provide important engineering data to validate the space worthiness of the novel gold-blackened thermal array detectors, and verify the thermal performance of the SBI's uncoated optics in a vacuum environment.

© 2004 COSPAR. Published by Elsevier Ltd. All rights reserved.

Keywords: Scientific ballooning; Solar Bolometric Imager; Solar photosphere; Solar physics

1. Introduction

Two 11-year cycles of space-borne radiometry have demonstrated that the total solar irradiance (and luminosity) increases by about 0.1% around activity maximum (Fröhlich and Lean, 1990). Analyses of this total irradiance record have shown that almost 95% of its variation is well correlated with the changing of the projected areas of dark sunspots and bright faculae and network (Fröhlich and Lean, 1990; Chapman et al., 1996). This strongly suggests that the measured luminosity variation can be attributed to the net effect on photospheric heat flow of the compensating contribu-

tions of these bright and dark magnetic structures (Foukal and Lean, 1988). However, it is still not clear whether the photometric effect of sunspots, faculae and network is actually *equal* or simply *proportional* to the measured radiometric fluctuations. Uncertain broadband photometric contrasts of spots, and especially faculae and network, currently present the main obstacle to improved modeling of total irradiance fluctuations. The bolometric contribution of faculae is currently uncertain by as much as a factor of two. Until this uncertainty is removed it cannot be considered proven that the compensating effects of bright and dark photospheric magnetic structures account entirely for measured solar luminosity variation. Demonstration of this equality is critical in determining whether the thermal blocking model (Foukal et al., 1983) provides an adequate physical explanation of solar irradiance variation, or whether more complex processes such as magnetic

* Corresponding author. Tel.: +1-240-228-8970; fax: +1-240-228-0386.

E-mail addresses: Pietro.Bernasconi@jhuapl.edu (P.N. Bernasconi), harry.eaton@jhuapl.edu (H.A.C. Eaton), pfoukal@world.std.com (P. Foukal), David.Rust@jhuapl.edu (D.M. Rust).

storage or enthalpy advection (Chapman, 1984; Schatten and Mayr, 1985) play a significant role. In addition, the possible existence of global changes that might dominate solar luminosity variation over climatologically important time scales is the most important unsolved problem in studies of solar luminosity variation (Shindell et al., 1999).

Here, we describe a balloon-borne solar telescope equipped with an innovative bolometric detector (Foukal and Libonate, 2001), capable of recording images with an angular resolution of about 5 arcsec in essentially total photospheric light. The Solar Bolometric Imager (SBI) will provide the first opportunity to bolometrically image brightness variations at the solar photosphere. Its flat spectral response from the ultraviolet to the infrared (like that of ACRIM) will directly provide the facular and network contribution to the total irradiance, and will complement the non-imaging space-borne radiometer measurements.

The three main objectives of the balloon-borne SBI are:

- To accurately measure (better than 10% per pixel) the bolometric contribution to the total solar irradiance of sunspots, faculae and enhanced network. This will help determine whether these structures can account for the rotational and 11-year variability of the total irradiance, or whether other mechanisms highly correlated with their area variation might contribute significantly. We note that the $\pm 10\%$ precision in photometry and the comparable accuracy in photometric contrast refer to the errors relative to the amplitude of the fluctuations in total irradiance caused by spots, faculae and network. Since these fluctuations are themselves of 0.1% amplitude relative to the total irradiance signal, our $\pm 10\%$ photometric goal represents $\pm 0.01\%$ precision relative to the total irradiance. This is similar to the precision achieved by the space borne radiometers.
- To search for other lower level inhomogeneities in photospheric heat flux uncorrelated with the photospheric magnetic structures themselves, and possibly associated with large-scale convective cells, meridional circulations, etc. Such inhomogeneities might prove more important over time scales longer than the 11-year cycle.
- To provide important engineering data to validate the space flight-reliability of the novel gold-blackened thermal array detector and to verify the thermal performance of the SBI uncoated optics in a vacuum environment.

2. System requirements

To achieve its science objectives, the SBI optical assembly must meet the technical requirements listed below:

- The telescope must be achromatic over the wavelength range from 0.28 (ultraviolet UV) to 2.6 μm (near infrared NIR) which includes about 96% of the total solar irradiance.
- The system spectral response must be constant to better than $\pm 10\%$ over the above mentioned range.
- The irradiance of the direct solar image at the focal plane must be reduced to within the acceptable range for the thermal-imaging detector. This is required because of the fixed detector integration time that limits the maximum acceptable intensity to 1 mW cm^{-2} .
- The system's angular resolution in the NIR must be sufficient to resolve structures of at least 10 arcsec in size. This is the characteristic size of the enhanced solar photospheric network, which is the smallest structure currently known to contribute significantly to the total irradiance variation. Excessive blurring would decrease the peak intensity of these structures, thus reducing the signal-to-noise ratio.
- The scattered light level must be sufficiently low to enable sunspot and facular contrast measurements of $\pm 10\%$ accuracy.
- The camera's photometric response must be sufficiently well understood and stable to enable photometric measurements of $\pm 10\%$ precision.

Other requirements more specifically related to the balloon flight are:

- The balloon must fly at altitudes higher than 24.5 km to avoid molecular band absorption from the Earth's atmosphere that would reduce the spectral coverage. Because of even more strict requirements dictated by the pointing system the goal altitude is actually about 36 km.
- Telescope and detector must be able to operate at the above mentioned altitude, where the air pressure is about 4 mBar, and at temperatures that can range from -50 (during the ascent phase) up to $+70$ °C (for the Sun facing surfaces). The telescope optics and mount must be able to handle the intense solar heating.

3. Optical design

The optical design of the SBI balloon instrument features of a 30-cm diameter F/12 Dall–Kirkham telescope with uncoated mirrors, followed by a filter wheel holding a set of neutral density filters with different attenuation factors and a 10 nm band-pass filter centered at 390 nm. Fig. 1 shows a schematic of the optics. The Dall–Kirkham design was chosen to provide inexpensively the required long focal length with a compact package necessary for a balloon flight. The telescope resolution at 0.28 μm is 0.2 arcsec and at 2.6 μm it increases to 2.2 arcsec. However, the detector pixel size is 2.86×2.86 arcsec per pixel (see next section) therefore

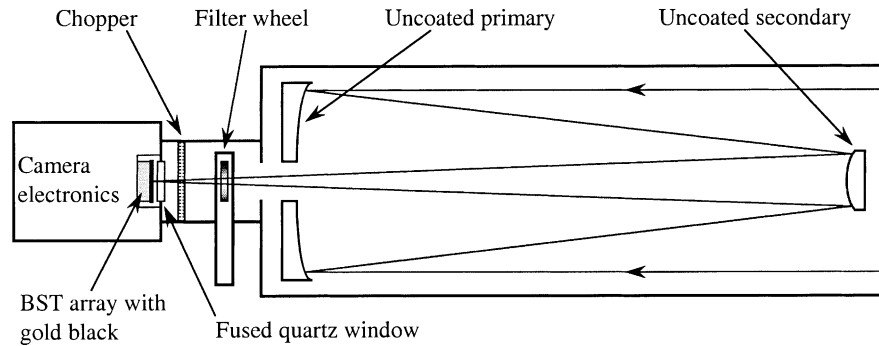


Fig. 1. Schematic of the optical system.

also in the NIR most of the point spread function peak lies within one pixel. This guarantees a nearly constant resolution over the entire portion of the spectrum measured by our bolometer.

Calculations and measurements indicated that bare (uncoated) Pyrex primary and secondary mirrors coupled with an Inconel-coated neutral density filter with fused quartz substrate provide both the appropriate attenuation and the best spectral flatness over a 0.28–2.6 μm spectral range. This range accounts for over 96% of the total solar irradiance and most of its percentage variability. Fig. 2 shows the predicted transmission of the optical system. The transmission curve varies by only $\pm 7\%$ over this range and is limited at short wavelengths by a local minimum in the reflectivity of Pyrex at 0.25 μm and at wavelengths greater than 2.6 μm by absorption features in the fused quartz.

The design includes a filter wheel. It will hold a set of four Inconel coated neutral density (ND) filters with attenuation factors of 1 and higher and a 10-nm interference filter centered at about 390-nm. The ND 1 filter will be the nominal filter used for the broadband imaging while the ND filters with higher attenuation factors will be used for calibration measurements. The 10-nm filter is centered above the CaKII line, which is particularly suitable to image the bright faculae and the enhanced network. This filter will provide a record of the location of these magnetic features during the flight.

All the materials used for the telescope are vacuum compatible, i.e., they do not out-gas continuously when exposed to vacuum. The telescope tube is made of carbon fiber, which exhibits very low thermal expansion. The tube and other components mounted inside the tube itself have been vacuum baked for 24 h to eliminate residual outgassing that may contaminate the mirrors surfaces during the flight. The secondary actuator motor, used to focus the image, is vacuum prepared and the focus mechanism is lubricated with a vacuum compatible lubricant.

4. Bolometric imager characteristics

4.1. Detector characteristics

The key component of the SBI is the bolometric imager, which has the unique capability to record images (320×240 pixels in size) in total light, i.e., with a flat photometric response from the UV to the NIR. The detector characteristics are described in detail in Foukal and Libonate (2001), therefore here we will only give a brief description.

The detector is composed of an array of 320×240 barium strontium titanate (BST) ferro-electric elements, each element $50 \times 50 \mu\text{m}$ in size. BST exhibits a strong temperature dependence of capacitance around its Curie

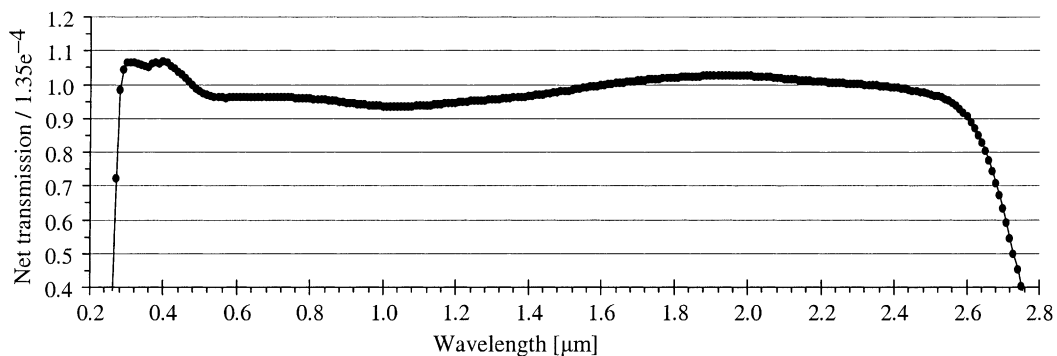


Fig. 2. Net optical transmission for the SBI system, calculated from measured values for the individual components (two uncoated Pyrex mirrors, one Inconel-coated ND 1.0 filter, and one fused-quartz detector window).

point (at about +30 °C). If exposed to IR radiation the elements produce a change in output current that is proportional to the radiation intensity. For the SBI we used a modified IR detector array based on this effect (Hanson, 1997), commercially available for night vision cameras.

For our 30 cm aperture F/12 telescope the image scale is 0.0573 arcsec per μm . Given the detector size, the image field of view is about 917×687 arcsec. Thus, a full disc image of the Sun can be obtained with a mosaic of ten single tiles, with the pattern 2-3-3-2, and with a considerable overlap between individual tiles.

To transform such a camera into a detector with flat response over the UV to NIR range, we deposited a thin ($\sim 30 \mu\text{m}$) layer of gold black on the monolithic light-receiving surface of the array. Gold-black films have a spectral absorptance that varies less than $\pm 1\%$ from 0.2 to beyond $3 \mu\text{m}$ (Advena et al., 1993). Therefore, such a film will uniformly redistribute the absorbed radiation in the above mentioned spectral range in the form of thermal emission and it will be detected by the underlying thermal IR BST imaging array. Fig. 3 shows that the measured hemispherical reflectance of a gold-blackened BST array is extremely flat over the spectral range between 300 and 1600 nm. This indicates that approximately 99% of the incident light in that range is absorbed. An image of a gold-blackened Raytheon BST detector array with fused quartz window used as a prototype for the SBI is shown in Fig. 4.

4.2. Camera operation

The detector elements are sensitive to temperature change but do not provide a DC response (the temperature signal is AC coupled). A chopper (with the shape of an Archimedes spiral) modulates the scene energy onto an AC carrier, normally at 30 Hz. Abrupt sensor output changes occur when the chopper blade exposes or blocks the source image energy. If the scene tem-

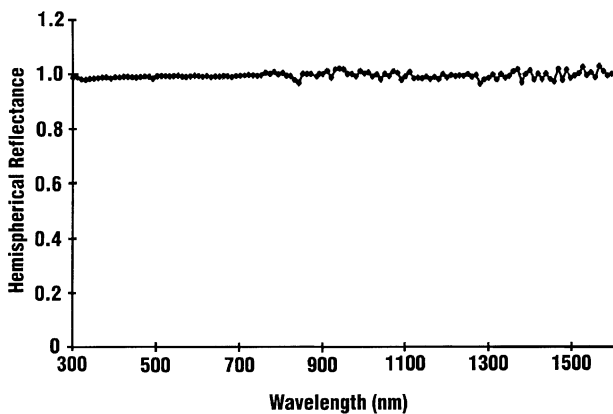


Fig. 3. Measured spectral reflectance (diffuse + specular) for a gold-blackened BST array.

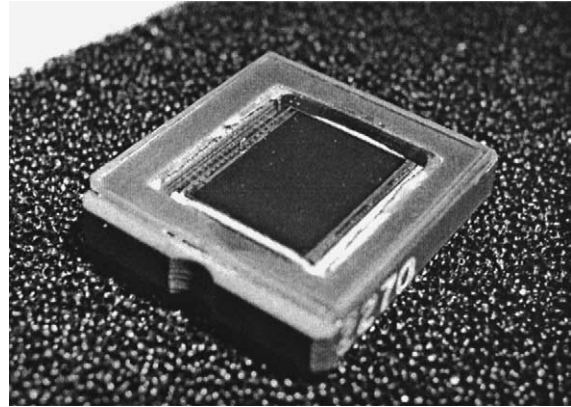


Fig. 4. A gold-blackened Raytheon ferro-electric array of the kind used in the SBI detector.

perature is higher than the chopper blade temperature, the pixel element will heat up when exposed and cool down when blocked. The opposite will occur if the scene temperature is colder than the chopper blade temperature, producing an apparent 180° phase shift in the signal, however this is a perfectly acceptable mode of operation for this imager chip.

The output from each pixel amplifier goes to a sample-and-hold circuit, and the output from the pixel multiplexer is the difference between the current pixel amplifier and the last held value. When the next adjacent pixel is read out, the previous pixel output is sampled and stored in its sample/hold circuit. This means that the output frames from the detector have alternating polarity. For example, if we define O_s the output signal when a pixel element is "looking" at the scene, and O_c the output signal when the chopper blade is in front of the same element, then the output signal $S(i)$ for that pixel for frame i (the i th cycle of the chopper blade) is given by:

$$S(i) = O_s - O_c + Z + \text{noise}, \tag{1}$$

where Z is an arbitrary signal offset. The output signal $S(i + 1)$ from the next frame would then be:

$$S(i + 1) = O_c - O_s + Z + \text{noise}. \tag{2}$$

By computing the difference between consecutive frames we obtain:

$$S(i) - S(i + 1) = 2(O_s - O_c) + \sqrt{2}\text{noise}, \tag{3}$$

thus eliminating the offset and reducing the noise.

5. Observing platform

For the balloon flight of the SBI we will use the same gondola and subsystems previously developed and employed for the Flare Genesis Experiment (FGE) project (Bernasconi et al., 2000). The FGE gondola has successfully endured a test flight in New Mexico (in 1994)

and two Antarctic flights (in January 1996: 21 days at float altitude, and in January 2000: 17days), carrying an 80-cm solar telescope at an average altitude of 36 km. During the past eight years the FGE gondola and its subsystems have undergone many improvements and upgrades and it is now a proven observing platform. It can guarantee a successful flight of the SBI without the need to design, manufacture and test a totally new gondola. Fig. 5 shows a schematic of the entire SBI system. The figure insert has an explanation of all the acronyms used in the diagram.

5.1. Gondola and power system

The basic payload dimensions are: 2 m wide, 1.5 m deep, and about 4.5 m high. The gondola is strong enough to support up to 2000 kg even under the 10 g pull that could be experienced at the end of a flight when the parachute inflates after the balloon cut-off. In addition,

it is rigid enough to allow the required telescope pointing stability.

The power system consists mainly of three elements: the battery stack, the power controller, and the voltage regulators. Meer Instruments of San Diego originally built the system. Because of the short duration of the SBI flight (<14 h), everything on board the gondola can be powered entirely by batteries. The absence of solar panels that can act as sails and add unwanted additional vibration modes will make pointing the SBI easier than pointing the FGE (see next sub section).

During the January 2000 flight of FGE the average power consumption was about 520 W. We expect a similar value for the SBI flight. We assume a minimum operation of 15 h, which includes 2 h before the launch and 13 h of actual flight. By including a 10% derating due to the below freezing temperature of operation, we expect a total power requirement of about 8.6 kW h. Commercially available Li-ion batteries have a perfor-

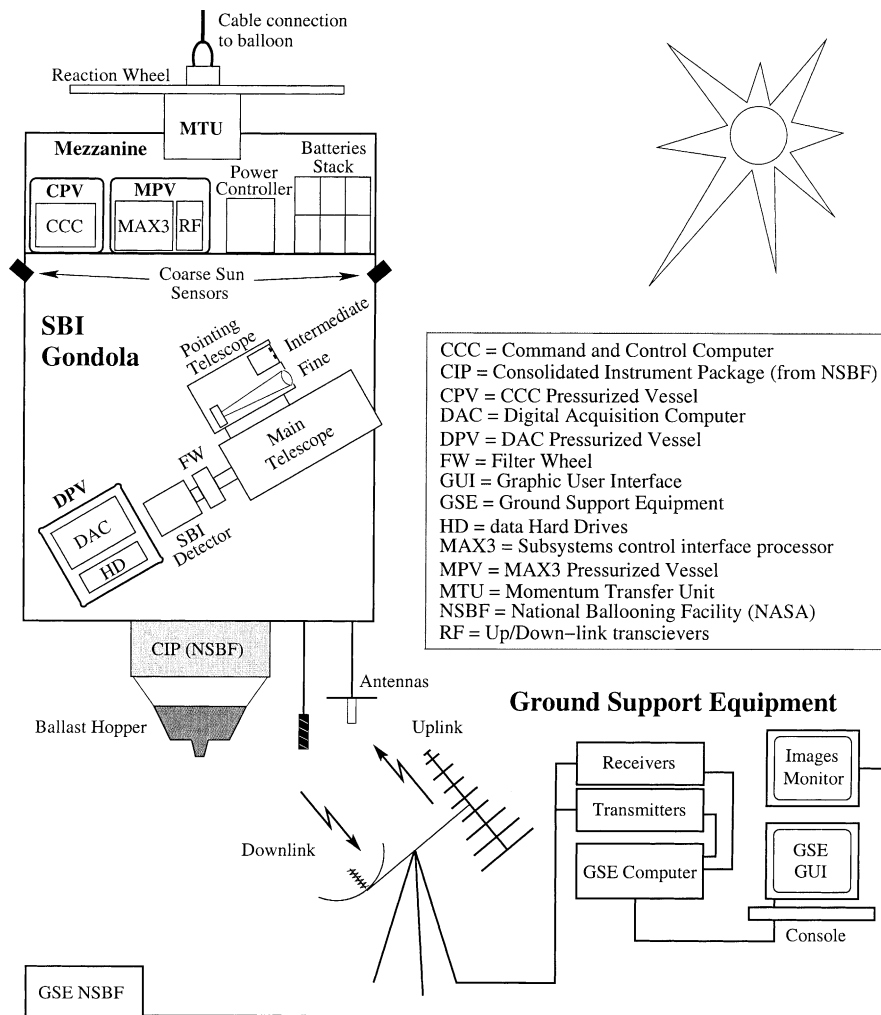


Fig. 5. Block diagram of the entire SBI system.

mance of about 130 W h per kilogram of weight, therefore we will require a total battery weight of about 66 kg. This means that the battery weight will not be of considerable impact on the total gondola weight.

The balloon itself and its control electronics will be provided by NASA's National Scientific Balloon Facility (NSBF) based in Palestine, Texas. NSBF will also be responsible for the payload launch and the balloon control.

5.2. Telescope mount

The telescope is mounted to the gondola frame on the elevation (pitch) axis drive shaft. It can pivot around this axis by a torque motor that connects the gondola frame to the telescope mount. During launch and landing, the telescope is stowed upright, protected by the frame. The gondola will turn in azimuth (yaw) by means of a reaction-wheel mounted on top of the gondola. The wheel is part of the Momentum Transfer Unit (MTU) which is the same developed for FGE (Bernasconi et al., 1999). The MTU serves to point the gondola in azimuth, to minimize disturbances introduced through the balloon suspension cable and to shift accumulated momentum from the reaction-wheel to the balloon. It acts also as the support and attachment point between the gondola and the parachute-balloon system.

In order to isolate the high frequency gondola jitter from the telescope we have developed a new mount equipped with a passive stabilizing system, which is basically composed of a spring, a mass, and a damper. Fig. 6 shows a schematic of the mount. Two cages are connected together via flex-pivot spring supports. The outer cage is directly attached to the elevation motor shaft and spins around the elevation axis. The telescope itself is connected to the inner cage also by means of two

flex-pivots that allow the telescope to rotate orthogonally to the elevation spin axis. Flex-pivots are weak torsional springs but they are capable of sustaining strong transversal and longitudinal forces. The spring-mass oscillation is passively damped with eddy currents: copper conductors move between strong permanent magnets and the interaction between the electrons in the conductor and the external magnetic field generates a force in the direction opposite to the velocity of the conductor. This new mount will allow stable pointing of the telescope, down to sub arcsec levels, even if the gondola is experiencing high frequency jitter of the order of several arc seconds.

5.3. Pointing system

The pointing control system is the same as the one successfully used by FGE (Bernasconi et al., 2000). It has three tracking states, each using a different and gradually more sensitive error sensing mechanism.

- Track-state 1: Coarse tracking. Four photodiode sensors (Coarse Sun Sensors) mounted at 90° intervals around the gondola provide the Sun's position in azimuth, while an encoder on the elevation shaft provides elevation information. A calculation of the ephemeris based on GPS time and position is used to find the initial solar elevation.
- Track-state 2: Intermediate tracking. Two detectors mounted on the front of a guiding telescope each consisting of a cylindrical lens mounted in front of a position-sensing photodiode are used to measure azimuth and elevation errors. The field of view of these detectors is approximately $\pm 20^\circ$ and they provide Sun-pointing to an accuracy of about 0.25° .
- Track-state 3: Fine tracking. A small guiding telescope rigidly mounted to the telescope mount outer

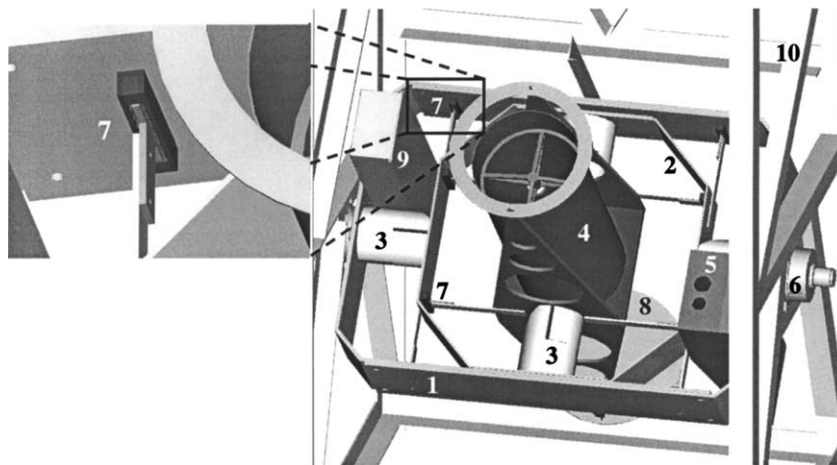


Fig. 6. Schematic of the telescope mount and other sub systems: (1) Mount outer cage; (2) Mount inner cage; (3) Flex-pivots; (4) Telescope; (5) Guiding telescope; (6) Elevation motor; (7) Damping elements; (8) Ring weight for counter balance; (9) Pressurized vessel housing the DAC computer; (10) Gondola frame.

cage produces the fine pointing error signals. The guiding telescope projects an image of the full solar disk (1 cm in diameter) onto a lateral-effect-diode (LED) used as a position sensor. The LED has a metal disk that occults the inner 90% of the Sun's image (the servo-loop always maintains the solar image on the center of the LED). An X–Y motion stage moves the LED in the image plane of the guiding telescope to affect offset pointing of the SBI Telescope from Sun center. When the occulting disk is fully illuminated, the pointing error is measured to 0.05 arcsec RMS.

The digital control system uses a two-pole, two-zero equalizer (equivalent to a PID controller with an extra pole available) to determine motor drive entirely from position errors and runs at a sample rate of 40 Hz. Each track state has four control coefficients per axis that can be adjusted in flight for optimum performance. Hand-off between the various track states is achieved by gradually blending the control output from one state to the next. This provides an extremely robust and fast acquisition of fine pointing.

5.4. Command control and communications

The command, control and communication system is also very similar to the one used for the FGE flights (Bernasconi et al., 2000). Although, some modifications in both hardware and software were necessary to account for the different subsystems used by SBI.

There are two main computers on-board: the Command and Control Computer (CCC) and the Digital Acquisition Computer (DAC). Both computers use a commercial ATX mother board with a 1GHz Pentium III. The CCC will run two separate processes: the Autonomous Control Executive (ACE) process and the Instrument Control (IC) process. The ACE is responsible for properly scheduling the operations performed by the gondola and to carry on the observational program. It can either operate totally autonomously or execute commands received directly from a ground control station via UHF radio link. The IC's main task is to provide a uniform interface for the ACE to a series of instrument subsystems. It also handles all the communications: it collects and transmits the housekeeping data and the I/O with all the instrument controllers. The DAC controls the SBI detector, and is responsible for handling the stream of images coming from the frame grabber. It can transfer the image data to one of the four 20 GB hard drives (of high shock type), and it can perform simple data manipulations if needed. It communicates directly to the CCC via an ethernet link. It can handle commands arriving directly from the ACE process and can deliver images to either the ACE or the IC (for example for a downlink).

The CCC, the DAC, the hard drives and other microprocessors are all commercial electronic products, thus not specifically designed to operate in a vacuum environment. They are all housed inside three pressurized vessels that maintain a stabilized pressure of 1 atm.

5.5. Flight profile

The SBI will be launched from the NSBF facility in Fort Sumner, New Mexico. The flight will last for about 13 h. Fig. 7 shows a sketch of a possible flight profile for SBI. In mid-September the Sun at Fort Sumner rises at about 6 a.m. and sets at approximately 6 p.m. Ideally, we would like to be at float altitude and start pointing at the Sun when it just, rises above the horizon. On average the balloon takes about 2 h to reach float altitude (above 30 km), therefore the ideal launch should take place at around 4 a.m. However, for safety reasons NSBF does not launch in the middle of the night, so we will probably launch at dawn or shortly thereafter.

Once an altitude of 26–27 km is reached, the engineering phase starts (point number 3 in Fig. 7). During this phase the pointing will be turned on and its performance tested and optimized, followed by a series of optimizations and calibrations of other subsystems, like for example the optimization of the telescope focus, and the recording of a flat field.

We expect the engineering phase to last about 2 h. The ACE will then execute a predetermined sequence of observations, but the sequence could be stopped or modified at any time from the ground. The main observing plan will probably include the recording of several mosaics of the Sun in total light (10 tiles, each tile is an average of 30 single frames), plus one or more mosaics with the 10 nm filter centered at 390 nm to

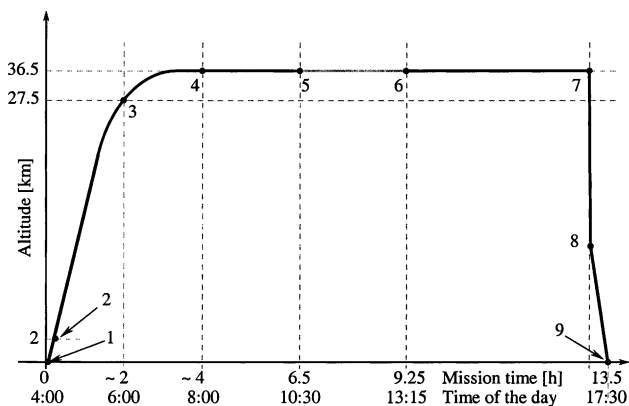


Fig. 7. Sketch of the SBI flight profile: (1) Launch (ideally 2 h before Sun rise); (2) The telescope is unstowed; (3) At sunrise the pointing system is turned on; (4) Start of the scientific observations; (5) The balloon starts to occult the Sun, observation are interrupted; (6) The Sun is no longer occulted by the balloon, observations are resumed; (7) Before sunset the mission is terminated, the gondola is detached from the balloon; (8) The parachute opens; (9) Landing at sunset.

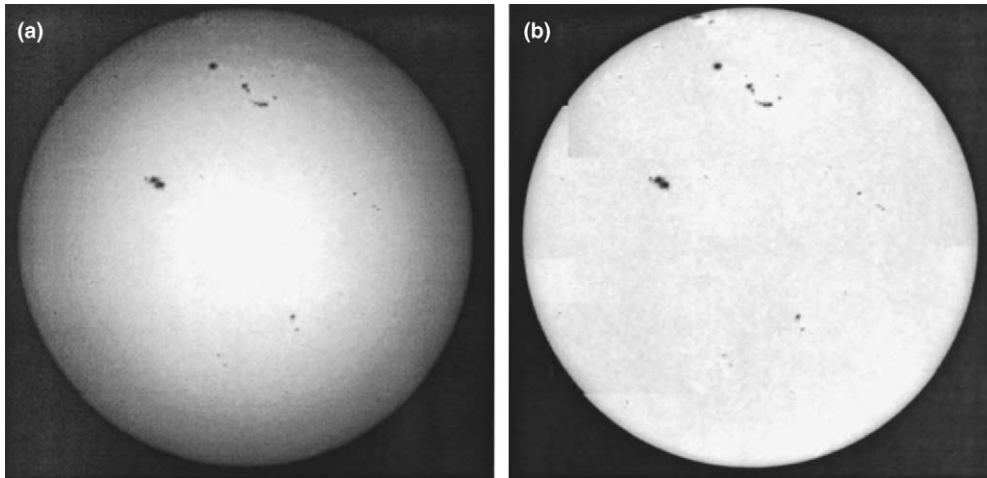


Fig. 8. Sun imaged in total light on September 24, 2002. The images were obtained by overlapping 10 bolometric frames recorded with the SBI detector and telescope during ground test observations at APL: (a) Mosaic before removal of the limb darkening; (b) After limb darkening removal. Sunspots and faculae are clearly visible. The spatial resolution of the images is about 5 arcsec. The artifacts present in the images are mostly due to imperfect flat fielding of the detector, which was not flight grade. The flight detector will be flat-fielded more precisely.

image the faculae and enhanced network. For about 3 h around noon time the observations will be interrupted because the balloon will occult the Sun (between points 5 and 6 in Fig. 7).

About 1 h before sunset, or when the balloon starts wandering too far from the launch site, the termination of the mission will be commanded. The ACE will stop all observations, stow the telescope, and shut down all the computers. Finally, a power off command will be sent from the ground and the instrument will be ready for the cut down (point 7 in Fig. 7).

6. Data analysis

6.1. Data reduction

After the flight the raw images will be first flat fielded and corrected for solar rotation. The flat field will be obtained in flight, by roughly pointing at Sun center, in a region absent from major active regions, and by averaging several frames together with the image slightly out of focus. Because of the large field of view the flat field will show some limb darkening effect, but this can be eliminated by fitting a theoretical limb darkening function to the image. About 30 frames will be recorded at each solar location. The corrected frames belonging to the same location will be co-aligned and averaged together, to improve the signal-to-noise ratio.

Following the preliminary reduction, the 10 images recorded at different solar locations will be merged to form a mosaic of the full disk. Subsequently, the limb darkening will be removed from the mosaic. Fig. 8 shows an example of full disc mosaics that can be obtained with the SBI. The images were recorded from the

ground during test observations with a development detector at the focus of the SBI telescope that will be used during the actual balloon flight.

6.2. Data products

From the SBI flight we expect to obtain the following data products:

- Full Disk broad band images of the solar photosphere with spectrally uniform response over the range from 0.28 to 2.5 μm and an angular resolution of about 5 arcsec. The objective is to obtain 0.1% photometric precision relative to the mean disk intensity at each pixel, so that we can measure the photometric contrast I_s/I_p to better than 10% accuracy (I_s = intensity of a structure, I_p = intensity of the photosphere). There are no requirements of absolute accuracy at time scales much longer than the duty cycle of recording one mosaic (~ 10 min).
- Narrow band images (10 nm band-pass at 390 nm) of the same scene showing bright magnetic structures with higher contrast than in wide band.

These images will allow creating maps of the photometric contrast I_s/I_p of spots faculae and network to the photosphere in wide band. The images will also help searching for other kinds of brightness inhomogeneities in the solar photosphere.

Acknowledgements

We are grateful to Graham Murphy, Marshal Jose, Sam Wilderson, and Rick Hildebrand for their contribution in the development of SBI. We also thank Scott

Libonate for his intense work in the early development of the gold-black bolometric detector. This work is funded by NASA under Grant NAG5-10998.

References

- Advena, D.J., Bly, V.T., Cox, J.T. Deposition and characterization of far-IR absorbing gold-blackening films. *Appl. Opt.* 32 (7), 1136–1144, 1993.
- Bernasconi, P.N., Rust, D.M., Murphy, G.A., Eaton, H.A.C. High resolution polarimetry with a balloon-borne telescope: the Flare Genesis Experiment, in: Rimmele, T.R., Balasubramaniam, K.S., Radick, R.R. (Eds.), *High Resolution Solar Physics: Theory, Observations and Techniques*, Astron. Soc. Pacific Conf. Series, vol. 183. San Francisco, California, pp. 279–287, 1999.
- Bernasconi, P.N., Rust, D.M., Eaton, H.A.C., Murphy, G.A. A balloon-borne telescope for high resolution solar imaging and polarimetry, in: Melugin, R.K., Röser, H.P., (Eds.), *Airborne Telescopes Systems*, Proc. SPIE, vol. 4014. Munich, Germany, pp. 214–225, 2000.
- Chapman, G. On the energy balance of solar active regions. *Nature* 308, 252–254, 1984.
- Chapman, G., Cookson, A., Dobias, J. Variations in total solar irradiance during solar cycle 22. *Geophys. Res. Lett.* 101, 13541–13548, 1996.
- Foukal, P., Fowler, L., Livshits, M. A thermal model of sunspot influence on solar luminosity. *Astrophys. J.* 267, 863–871, 1983.
- Foukal, P., Lean, J. Magnetic modulation of solar luminosity by photospheric activity. *Astrophys. J.* 328, 347–357, 1988.
- Foukal, P., Libonate, S. Total-light imager with flat spectral response for solar photometric measurements. *Appl. Opt.* 40 (7), 1138–1146, 2001.
- Fröhlich, C., Lean, J. The Sun's total irradiance: cycles trends and related climate change uncertainties since 1976. *Geophys. Res. Lett.* 25, 4377, 1990.
- Hanson, C. Hybrid pyroelectric–ferroelectric bolometer arrays, in: *Uncooled IR Imaging Arrays and Systems*Krase, P., Skatrud, D. (Eds.), *Semiconductors and Semimetals*, vol. 47. Academic, New York, pp. 123–173, 1997.
- Schatten, K., Mayr, H. On the maintenance of sunspots – an ion hurricane mechanism. *Astrophys. J.* 299, 1051–1062, 1985.
- Shindell, D., Rind, D., Balachandran, N., Lean, J., Lonergan, P. Solar cycle variability, ozone, and climate. *Science* 284, 305–308, 1999.